# Retrospective Study of $^{18}$F-FDG PET/CT in the Diagnosis of Inflammatory Breast Cancer: Preliminary Data

Selin Carkaci[1], Homer A. Macapinlac[2], Massimo Cristofanilli[3], Osama Mawlawi[4], Eric Rohren[2], Ana M. Gonzalez Angulo[3], Shaheenah Dawood[3], Erika Resetkova[5], Huong T. Le-Petross[1], and Wei-Tse Yang[1]

*[1]Department of Diagnostic Radiology, University of Texas M.D. Anderson Cancer Center, Houston, Texas; [2]Department of Nuclear Medicine, University of Texas M.D. Anderson Cancer Center, Houston, Texas; [3]Morgan Welch IBC Research Program and Clinic, Department of Breast Medical Oncology, University of Texas M.D. Anderson Cancer Center, Houston, Texas; [4]Department of Medical Physics, University of Texas M.D. Anderson Cancer Center, Houston, Texas; and [5]Department of Pathology, University of Texas M.D. Anderson Cancer Center, Houston, Texas*

Our objective was to retrospectively evaluate $^{18}$F-FDG PET/CT in the initial staging of inflammatory breast cancer (IBC). **Methods:** The institutional review board waived informed consent and approved this study, which was compliant with the Health Insurance Portability and Accountability Act. The cases of 41 women with a mean age of 50 y (range, 25–71 y) and newly diagnosed IBC who underwent $^{18}$F-FDG PET/CT at diagnosis were retrospectively reviewed. All PET/CT images were analyzed visually and semiquantitatively by 2 physicians. The maximum standardized uptake value in the primary breast, regional nodes (axillary, subpectoral, supraclavicular, internal mammary), and extranodal regions was documented. The accuracy of PET/CT image interpretation was assessed by histopathologic analysis, if available; concurrent or subsequent imaging findings (contrast-enhanced CT, contrast-enhanced MRI, sonography, or PET/CT follow-up); or clinical follow-up. **Results:** All patients presented with unilateral IBC. PET/CT showed hypermetabolic uptake in the skin in all patients, in the affected breast in 40 (98%), in the ipsilateral axillary nodes in 37 (90%), and in the ipsilateral subpectoral nodes in 18 (44%). Twenty patients (49%) were found to have distant metastases at staging, 7 (17%) of whom were not known to have metastases before undergoing PET/CT. Disease sites included bone, liver, contralateral axilla, lung, chest wall, pelvis, and the subpectoral, supraclavicular, internal mammary, mediastinal, and abdominal nodes. **Conclusion:** PET/CT should be considered in the initial staging of IBC, as the technique provided valuable information on locoregional and distant disease in this preliminary retrospective study.

**Key Words:** breast neoplasm; inflammatory breast cancer; $^{18}$F-FDG PET/CT; mammography; sonography; CT regional adenopathy

**J Nucl Med 2009; 50:231–238**
DOI: 10.2967/jnumed.108.056010

Received Jul. 16, 2008; revision accepted Nov. 20, 2008.
For correspondence or reprints contact: Wei-Tse Yang, 1515 Holcombe Blvd., Houston, TX 77030-4009.
E-mail: wyang@di.mdacc.tmc.edu


Inflammatory breast cancer (IBC) is a rare but aggressive manifestation of primary breast cancer, with characteristics of rapidly proliferating disease. The criteria for clinical diagnosis include erythema, edema involving more than two thirds of the breast, *peau d'orange* changes, breast enlargement, warmth, tenderness, and breast induration on palpation (*1*). IBC constitutes 1%−2% of primary breast cancers in the United States, but its incidence is increasing (*2*). Approximately 20% of patients with IBC have gross distant metastases at the time of diagnosis, and the mean 5-y overall survival rate of IBC patients who have undergone current multidisciplinary therapy is 20%−40%, with a median survival of 12–36 mo (*3–5*).

The standard treatment for IBC is neoadjuvant chemotherapy followed by modified radical mastectomy and radiation therapy. Multiple investigations, including chest radiography, whole-body bone scintigraphy (WBS), CT, and MRI, are conducted to exclude distant metastasis before therapy.

Integrated $^{18}$F-FDG PET and PET/CT have an emerging role in evaluating patients with malignant tumors. $^{18}$F-FDG PET/CT has the ability to coregister both anatomic and functional information (*3,6*). $^{18}$F-FDG PET and $^{18}$F-FDG PET/CT have been evaluated for detecting and diagnosing primary breast cancers, staging locoregional and distant sites, and monitoring response to neoadjuvant chemotherapy (*7–17*). The potential limitation of $^{18}$F-FDG PET in breast imaging is the detection of microscopic disease and the detection of disease in lesions smaller than 1 cm. Therefore, $^{18}$F-FDG PET is not routinely used in the staging work-up of patients with stage 1 or early stage 2 disease. To our knowledge, the role of $^{18}$F-FDG PET/CT in staging IBC has been scarcely addressed in the medical literature (*3*), compared with staging of other diseases (*18–20*). The purpose of this retrospective study was to evaluate the accuracy of $^{18}$F-FDG PET/CT in the initial staging of IBC.

## MATERIALS AND METHODS

### Patients

One of several authors searched the PET/CT database to identify consecutive patients who had been diagnosed with IBC at the University of Texas M.D. Anderson Cancer Center between July 2005 and July 2007 and had PET/CT data available for review. Patients were selected on the basis of standard clinical criteria for IBC as documented from the clinical charts. These criteria included erythema, edema involving more than two thirds of the breast, *peau d'orange* changes, or breast induration on palpation. Patients who had undergone neoadjuvant chemotherapy or surgery before PET/CT were excluded. A retrospective review was then performed to document patient age, clinical and imaging findings (including mammography, breast ultrasound or MRI, WBS, chest radiography, and chest and abdominal CT), and histopathologic findings when available. The institutional review board waived informed consent and approved the retrospective review, which was compliant with the Health Insurance Portability and Accountability Act (*21*).

### Imaging and Review

$^{18}$F-FDG PET/CT was performed using a Discovery ST camera (GE Healthcare) in combination with the CT component of an 8-slice LightSpeed scanner (GE Healthcare). The patients had been positioned supine in the PET/CT device, with their arms raised, and had fasted for at least 6 h before the $^{18}$F-FDG injection. Normal fasting blood glucose levels of less than150 mg/dL were a standard requirement for imaging in all patients. An intravenous injection of 555–629 MBq (15–17 mCi) of $^{18}$F-FDG had been administered in the arm or central venous catheter on the side opposite the cancer, and 2-dimensional emission scans had been acquired at 3 min per field of view 60–90 min after the $^{18}$F-FDG injection. PET images had been reconstructed using standard vendor-provided reconstruction algorithms. Noncontrast-enhanced CT images had been acquired in helical mode (speed, 13.5 mm/rotation) from the base of the skull to the mid thigh during suspended mid expiration at a 3.75-mm slice thickness, 120 kVp, 300 mAs, and a 0.5-s rotation.

The CT, PET, and coregistered PET/CT images were reviewed in all standard planes with maximum-intensity whole-body coronal projection images on an AW workstation (GE Healthcare). All images were retrospectively reviewed again jointly by 2 physicians, who had details on the patients' clinical history but did not know the results of other imaging studies and clinical follow-up.

The PET scans were analyzed visually and semiquantitatively. $^{18}$F-FDG uptake was considered to be abnormal on visual analysis when uptake in the region of the primary tumor was substantially higher than that in the background in the contralateral breast or axilla. The highest recorded $^{18}$F-FDG uptake was semiquantitatively analyzed, after being corrected for radioactive decay, according to the following formula: maximum standardized uptake value (SUV) = maximum voxel activity within the area of interest (MBq/mL)/injected dose (MBq)/body weight (g). The maximum SUVs in the primary breast, regional axillary nodes, subpectoral nodes, supraclavicular nodes, internal mammary nodes, and distant solid and visceral organs were documented. Interpretation was based primarily on qualitative interpretation (visual assessment of signal intensity by comparison with physiologic structures such as liver, bowel, and background soft tissue) and agreement between 2 readers. The maximum SUV was documented for each lesion designated as abnormal. Breast lesions were categorized as unifocal, multifocal, or multicentric. CT images were reviewed using lung, soft-tissue, and bone windows. The CT criteria for malignant nodes included a short-axis diameter of more than 1 cm.

### Histopathologic Analysis

One dedicated breast pathologist reviewed the hematoxylin- and eosin-stained slides of core biopsy, excisional biopsy, or mastectomy specimens to determine histologic tumor type, histologic grade, presence of angiolymphatic invasion, and presence of dermal lymphatic invasion. Histologically, the tumors were classified as invasive ductal carcinoma, invasive lobular carcinoma, invasive metaplastic carcinoma, or a combination of these types. Invasive tumors were graded on the basis of the Nottingham grading system (the Elston–Ellis modification of the Scarff–Bloom–Richardson system), which is a combined score based on an evaluation of tubule formation, mitotic count, and nuclear pleomorphism, as described previously (*22*).

In the staging of ipsilateral regional nodal basins for breast cancer, N3 disease is defined by involvement of a node in the subpectoral, internal mammary, or supraclavicular region (*23*). Therefore, a patient with multiple sites of ipsilateral nodal involvement was subjected to biopsy of a single (the highest) nodal station instead of biopsy of multiple nodal regions to confirm metastases.

### Data Analysis

The accuracy of PET/CT image interpretation was assessed by histopathologic analysis, if available; concurrent or subsequent imaging findings (contrast-enhanced CT, contrast-enhanced MRI, sonography, or follow-up PET/CT); or clinical follow-up. Results were considered true-negative when PET/CT correctly classified a benign lesion and no evidence of disease was documented during 1 y of clinical or imaging follow-up. Results were considered false-negative when PET/CT classified histologically confirmed cancer as benign or when PET/CT classified highly suggestive correlative imaging findings (progressive $^{18}$F-FDG uptake or increasing size of lesions) as benign. Results were considered false-positive when PET/CT classified histologically benign findings as cancer or when PET/CT classified benign findings on correlative imaging as cancer. Results were considered true-positive when PET/CT classified histologically malignant findings as cancer or when PET/CT classified malignant findings on correlative imaging as cancer. Correlative imaging in the absence of histology was performed according to the system involved: plain radiography, WBS, and MRI were used to confirm the presence or absence of musculoskeletal lesions; contrast-enhanced CT or MRI of the abdomen, of abdominal lesions (e.g., liver or spleen); chest radiography or chest CT, of pulmonary, pleural, or mediastinal lesions; and chest, abdominal, or pelvic CT or MRI, of nodal disease measuring more than 1 cm (and more than 0.7 cm in the internal mammary chain). Data were recorded, and data analysis was performed on both per-patient and per-disease-site bases. Data were analyzed with SPSS, version 11 (SPSS Inc.).

## RESULTS

Of 95 patients referred to our institution with IBC from July 2005 to July 2007, 41 newly diagnosed patients with unilateral primary IBC who had PET/CT data available for review were included in our study. The remaining 54 patients had metastatic IBC and were not included in the study. The mean age of the patients at diagnosis was 50 y (range, 25–71 y). Twenty-four women were premenopausal, and 17 were postmenopausal (6 of whom were on hormone replacement ther-

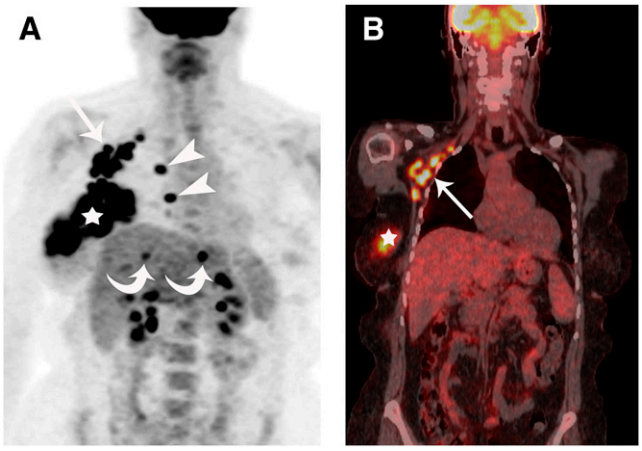


**FIGURE 1.** A 52-y-old woman with biopsy-proven right IBC. (A) Maximum-intensity-projection reconstruction of CT-attenuation-corrected PET image shows global hypermetabolic uptake in right breast (star), right subpectoral nodes (arrow), and right internal mammary nodes (arrowheads) and bilobar liver metastases (curved arrows). (B) Coronal PET/CT shows right subpectoral (arrow) and right breast (star) uptake.

apy). One patient had a history of prior contralateral breast cancer. The left breast was affected in 22 patients (54%), and the right breast in 19 patients (46%).

### Locoregional Disease (Breast and Regional Lymph Nodes)

All patients presented with swelling and skin changes (rash, erythema, or discoloration). A palpable mass was not evident on physical examination in 26 patients (63%). $^{18}$F-FDG PET/CT showed hypermetabolic uptake in the affected breast in 40 patients (98%), with multicentric distribution in 28 (68%) (Fig. 1). The mean SUV was 11.4 (range, 2.5–30.6). All patients had skin thickening that demonstrated hypermetabolic uptake and a mean SUV of 5.2 (range, 2.5–29.0). Nineteen patients (46%) had biopsy-proven skin invasion. In 1 patient, hypermetabolic skin thickening was noted, but no $^{18}$F-FDG–avid lesion was identified within the affected breast. No discrete mass was identified sonographically or mammographically in this patient. The final pathologic finding in this patient was invasive ductal carcinoma with associated ductal carcinoma in situ. The predominant histologic type was invasive ductal cancer (36 patients [88%]). Thirteen patients (32%) had mixed invasive ductal carcinoma and ductal carcinoma in situ. The histologic grade was intermediate (20 [49%]) or high (21 [51%]).

PET/CT did not detect grade 3 ductal carcinoma in situ in the contralateral breast in 1 patient with IBC; the ductal carcinoma in situ presented as an area of pleomorphic calcifications measuring 8 cm on mammography and as a 9-cm asymmetric, segmental, nonmasslike enhancement on MRI. In another patient, PET/CT demonstrated hypermetabolism in a 3.5-cm mass (SUV, 7.5) in the contralateral breast that was highly suggestive of malignancy on both mammography and sonography. Biopsy was not performed because the patient had presented with widely disseminated metastasis.

The ipsilateral regional nodal basins, including the axillary, subpectoral, supraclavicular, and internal mammary regions, were evaluated in 41 patients, giving a total of 164 nodal regions. Biopsy confirmation of metastasis was available for 38 nodal stations in 41 patients (Table 1). Three patients (7%) had no regional nodal metastasis at the time of initial staging (N0). Fourteen patients (34%) had metastasis to the axillary lymph nodes (N1 or N2), and 24 patients (59%) had metastasis to the subpectoral, internal mammary, or supraclavicular lymph nodes: N3 disease according to the American Joint Committee on Cancer Staging (Figs. 1 and 2) (*23*). PET/CT detected axillary metastasis in 37 patients (90%). Of these, biopsy confirmation was available for 29 (71%). Thirty-one of 41 patients (76%) presented with clinically palpable ipsilateral axillary nodes. One false-negative finding involved a 0.7-cm axillary lymph node that did not show hypermetabolism on $^{18}$F-FDG PET/CT but showed carcinoma on sonography-guided fine-needle aspiration biopsy.

**TABLE 1.** PET/CT Findings for Ipsilateral Regional Lymph Nodes in 41 Patients with IBC

| Site | Patients with uptake | Mean size* (cm) | Mean SUV* | Biopsy | Correlative imaging | | | False-negative | False-positive |
|---|---|---|---|---|---|---|---|---|---|
| | | | | | Total | Biopsy of 1 nodal site† | Distant metastases, no biopsy‡ | | |
| Axillary | 38 (90%) | 2.5 (0.7–4.6) | 11.7 (2.5–36) | 29 (71%)§ | 9 (22%) | 6 (15%) | 3 (7%) | 1 | 0 |
| Subpectoral | 19 (44%) | 1.3 (0.7–2.5) | 11 (2.5–34) | 4 (10%) | 15 (34%) | 8 (20%) | 7 (14%) | 1 | 0 |
| Supraclavicular | 10 (15%) | 1.4 (0.7–2.0) | 6.8 (3.7–12.6) | 5 (12%)‖ | 5 (12%) | 2 (5%) | 3 (7%) | 4 | 0 |
| Internal mammary | 9 (22%) | 1.2 (0.8–1.6) | 7.8 (3.7–13.7) | 0 | 9 (22%) | 6 (15%) | 3 (7%) | 0 | 0 |

*Range is in parentheses.
†These patients had abnormal regional lymph nodes at multiple sites, all of which were regarded as metastatic after biopsy confirmed that 1 site—axillary, subpectoral, or supraclavicular—was metastatic.
‡In these patients, no biopsy was performed in view of distant metastases.
§One patient had positive biopsy findings and negative PET/CT findings.
‖Four patients had positive biopsy findings and negative PET/CT findings.

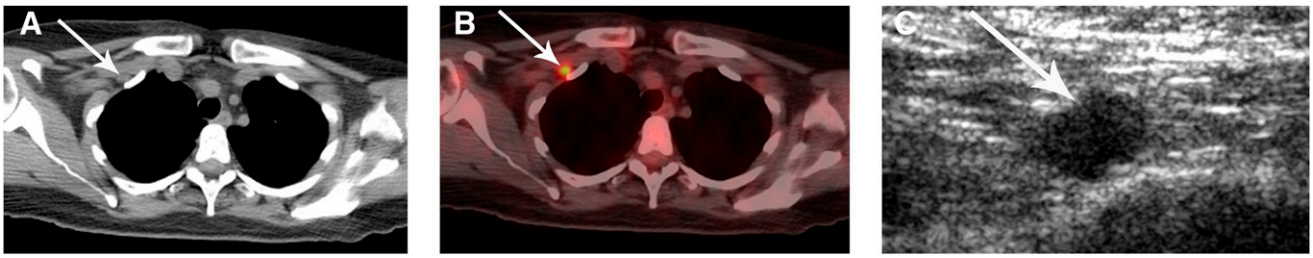


**FIGURE 2.** A 53-y-old woman with biopsy-proven right IBC. (A and B) Axial thoracic CT (A) and PET/CT (B) show solitary hypermetabolic, 1-cm medial subpectoral lymph node (arrow). (C) Transverse ultrasound shows abnormal solid, irregular, hypoechoic lymph node in medial subpectoral region (arrow). Ultrasound-guided fine-needle aspiration confirmed metastasis.

Up to 44% of patients had subpectoral (N3), 22% internal mammary, and 15% supraclavicular nodal involvement. Biopsy confirmation of nodal disease was available in 30%, 17%, and 15% of patients for the subpectoral, internal mammary, and supraclavicular regional nodal basins, respectively, when we summed the number of patients who had direct biopsy and the number who had multiple regional nodal involvement and biopsy of at least 1 site of N3 disease (Table 1).

### Distant Metastasis

Twenty patients (49%) had distant metastasis found on PET/CT at initial staging (Table 2); 11 (27%) of these patients had disease in multiple sites, and 9 (22%) had disease in a single site. Biopsy confirmation was available for 7 sites in 7 patients (17%), and 2 of these sites were false-negative on PET/CT. Of the 13 patients without biopsy confirmation, 6 had a single disease site and 7 had multiple disease sites. The most common sites of metastasis were the mediastinal lymph nodes (10 [24%]) (Fig. 3), bone (9 [22%]) (Fig. 3), and liver (6 [15%]) (Fig. 1; Table 3).

Four of 41 patients (10%) presented with clinical symptoms suggesting metastatic disease (2 had bone pain, 1 had palpable contralateral axillary nodes, and 1 had a palpable ipsilateral soft-tissue mass extending to the abdomen) that was confirmed on PET/CT. Seven of 41 patients (17%) did not have metastases suspected at clinical examination or baseline imaging and showed distant metastases on PET/CT. These 7 patients included 4 with negative WBS findings and positive PET/CT findings in the bone confirmed on correlative MRI and 3 with negative chest radiography findings and positive PET/CT findings in the supraclavicular and mediastinal regions. Biopsy confirmed metastasis of the contralateral supraclavicular node in 1 patient. The remaining 9 of 41 patients (22%) had distant metastatic disease visible on both PET/CT and routine staging studies including WBS, CT, and chest radiography.

PET/CT detected bone metastasis in 9 patients (22%) (5 lytic, 3 mixed lytic/sclerotic, and 1 bone marrow) (Fig. 3). The diagnosis of bone metastasis was confirmed by supplementary imaging (CT, WBS, and MRI) and follow-up in all patients. PET/CT and WBS were performed on 2 patients; PET/CT and MRI of the spine on 4; and PET/CT, WBS, and MRI on 3. In 1 patient with bone marrow metastasis, PET/CT detected a single, lytic, hypermetabolic lesion, whereas MRI showed multiple lesions throughout the axial skeleton. WBS did not identify 2 lytic lesions and 1 mixed metastasis in 3 of the 9 patients (33%).

PET/CT detected liver metastasis in 6 patients (15%). Three patients had unilobar and 3 had bilobar liver metastases (Fig. 1) confirmed by correlative imaging. Three patients had $^{18}$F-FDG–avid abdominal lymph node metastases (mesenteric and internal iliac) confirmed by correlative imaging and follow-up.

PET/CT detected pulmonary parenchymal metastases in 2 patients (5%) (Fig. 3); these findings were confirmed by correlative imaging and follow-up. One patient had uptake in multiple pulmonary nodules, visible on chest radiography and chest CT, with a mean diameter of 1 cm. One patient had a single 1.4-cm $^{18}$F-FDG–avid pulmonary nodule. This was considered a metastasis rather than a primary lung carcinoma because of biopsy-proven metastasis in the contralateral axilla. There were 2 false-negatives in 2 patients; subcentimeter pulmonary metastases did not show $^{18}$F-FDG uptake in either of these 2 patients. Both patients had metastases in multiple sites, including liver and bone. One patient had a calcified pulmonary nodule, characteristic of a granuloma, that showed increased $^{18}$F-FDG uptake and was categorized as benign. PET/CT detected metastases to the mediastinal lymph nodes in 10 patients (24%) (Fig. 3). There was 1 false-positive cardiophrenic angle mass with an SUV of 5.3 that was found to be reactive lymphoid tissue on CT-guided biopsy (Fig. 4). Of 2 biopsy-proven pleural metastases, 1 showed $^{18}$F-FDG uptake, with an SUV of 2.5. Another patient had a malignant effusion that did not show $^{18}$F-FDG uptake but revealed scant malignant cells on aspiration.

PET/CT detected contralateral lymph node metastases in 7 patients (17%). Biopsy confirmation was available for 4 sites in 4 patients (10%). There was 1 false-positive contralateral axillary lymph node, measuring 2 cm, that had an SUV of 5.9 and showed benign findings on biopsy (Table 3). There was 1 false-negative result for a 2-cm contralateral axillary lymph node metastasis that had an SUV of 1.9.

**TABLE 2.** Correlation Between PET/CT Findings of Distant Metastases and the Findings of Biopsy and Other Imaging Modalities in 20 Patients with IBC

| | PET/CT findings | | | | | | | | | | | |
|---|---|---|---|---|---|---|---|---|---|---|---|---|
| | | Chest | | | Abdomen | | Contralateral LNs | | | | | |
| Patient no. | Musculoskeletal | Pulmonary | Pleural | Mediastinal | Liver | LNs | Axillary | Subpectoral | Internal mammary | Supraclavicular | Biopsy | Correlative imaging |
| 1* | | | | + | | | | | | + | Pos (supraclavicular) | CT, FU |
| 2† | + | | | | | | | | | | 0 | MRI |
| 3 | + | | | | + | | | | | | 0 | CT, WBS |
| 4 | | | | + | | | + | + | | + | 0 | FU |
| 5† | | | | | | | | | | + | Pos (supraclavicular) | US, FU |
| 6 | | | | + | | | + | | | | Pos (axillary) | CT, FU |
| 7 | | | | | | | − (FN) | | | | Pos (axillary) | US, CT |
| 8 | | | | | + | | | | | | 0 | CT |
| 9* | + | | | | | | | | | | Pos (chest wall) | US, CT |
| 10* | + | + | | + | | | | | + | | 0 | CT, WBS, FU |
| 11† | | | | + | | | | | | | 0 | CT |
| 12 | + | − (FN) | | | + | | | + | | | 0 | CT, WBS, FU |
| 13 | | | − (FN) | + | + | | + | | | | Pos (pleural) | CT |
| 14* | + | | + | + | + | + | | | | | 0 | CT, WBS |
| 15† | + | | | | | | | | | | 0 | MRI |
| 16† | + | | | + | | + | + (FP) | | | | Neg (axillary) | CT, MRI |
| 17 | + | − (FN) | | + | + | | | | + | | 0 | CT, WBS, FU |
| 18 | | + | | | | | + | | | | Pos (axillary) | CT, US |
| 19† | + | | | | | | | | | | 0 | CT |
| 20† | | | | + | | | | | | | 0 | FU |

*Patients who presented with clinical features suggestive of metastases.

†Patients who did not have clinical suspicion or imaging evidence of metastases before PET/CT.

LNs = lymph nodes; + = positive on PET/CT; Pos = positive; FU = follow up with PET/CT; US = ultrasound; − = negative on PET/CT; FN = false-negative; FP = false-positive; Neg = negative.

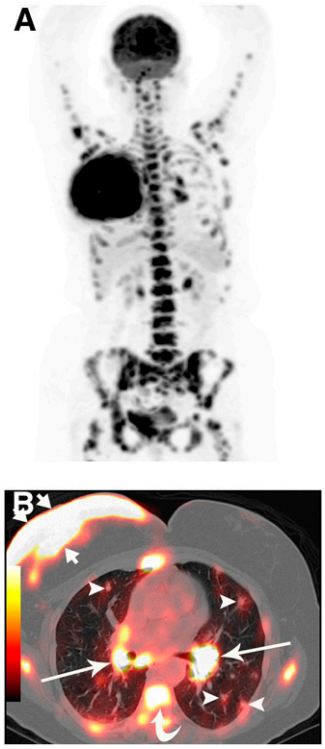


**FIGURE 3.** A 52-y-old woman with biopsy-proven right IBC. (A) Maximum-intensity-projection reconstruction of CT-attenuation-corrected PET image shows multiple areas of $^{18}$F-FDG uptake consistent with extensive metastasis. (B) Axial PET/CT shows $^{18}$F-FDG uptake in right breast, with associated diffuse skin thickening (short arrows), and uptake in bilateral hilar nodes (long arrows), axial skeleton (curved arrow), and pulmonary nodules (arrowheads).

## DISCUSSION

To our knowledge, this was the largest study describing the role of PET/CT in staging IBC. PET/CT showed hypermetabolic uptake in the affected breast in all but 1 patient in this study. These findings are similar to the results of Baslaim et al. and van der Hoeven et al. (*24,25*) but differ from those results regarding the value of $^{18}$F-FDG PET in early breast cancer (stages 1 and 2), for which PET has shown a lower accuracy (*18,26,27*), likely secondary to the low tumor volume. Diffuse hypermetabolic skin thickening was noted in all patients and is a unique feature of IBC that is infrequent in all other subgroups of breast cancer.

The single false-negative case in which PET/CT did not show uptake within the affected breast was found to be invasive and in situ ductal carcinoma at pathologic examination. No discrete mass was identified on sonography or mammography in this patient. PET/CT did not show uptake in a grade 3 ductal carcinoma in situ in the contralateral breast of 1 patient. This carcinoma had presented as pleomorphic calcifications on mammography and as an asymmetric, segmental, nonmasslike enhancement on MRI, measuring up to 9 cm. The absence of $^{18}$F-FDG uptake in the breast does not exclude the presence of malignancy, particularly early noninvasive malignancy, or well-differentiated primary breast cancers including ductal carcinoma in situ, tubular carcinoma, and invasive lobular carcinoma (*17,26,27*).

An unusually high percentage of axillary node involvement (90%) was noted in our study. This result can be attributed to the large size (mean, 2.5 cm) of the affected lymph nodes. The high sensitivity in the detection of axillary nodal metastases in our study is distinct from prior reports that described varied sensitivity in the detection of axillary nodal disease ranging from 20% to 85% (*11,12,28*). These findings likely reflect differences in biology between IBC (*29–32*) and breast cancer of lower stage (*11,12,28*)—differences that are associated with a higher prevalence of axillary nodal disease in IBC patients and are underscored by the high percentage of associated ipsilateral regional nodal (N3) disease in these patients.

There was 1 false-negative finding in our study, involving a 0.7-cm axillary node with an SUV of 2.0. The inability of PET to detect micrometastases may in part be due to intrinsic tumor characteristics (*13*). The majority of false-negative findings in our investigation involved small lesions (<1.3 cm), which are susceptible to partial-volume effects and the underestimation of lesion uptake due to the limited spatial resolution of the PET scanner (*11,33,34*). The CT component of commercially available hybrid PET/CT scanners can potentially resolve the problem of partial-

**TABLE 3.** PET/CT Findings of Distant Metastasis in 41 Patients with IBC

| Site of metastasis | Patients (*n*) | Patients with uptake (*n*) | Mean SUV* | Patients with biopsy confirmation (*n*) | Patients with correlative imaging and follow-up (*n*) | False-positive | False-negative |
|---|---|---|---|---|---|---|---|
| Bone | 9 | 9 | 13.4 (5.8–24.6) | 0 | 9 | 0 | 0 |
| Liver | 6 | 6 | 9 (4.9–12.7) | 0 | 6 | 0 | 0 |
| Abdominal nodes | 3 | 3 | 8.3 (2.5–10.2) | 0 | 3 | 0 | 0 |
| Pulmonary | 4 | 2 | 12.4 (10.3–14.4) | 0 | 4 | 0 | 2 |
| Pleural | 2 | 1 | 2.5 | 2 | 0 | 0 | 1 |
| Mediastinal lymph nodes | 10 | 11 | 8.8 (3.6–17.3) | 1 | 10 | 1 | 0 |
| Soft tissue | 1 | 1 | 4.3 | 1 | 0 | 0 | 0 |
| Contralateral lymph nodes | 7 | 7 | | 4 | | | |
| Axillary | 5 | 5 | 4.4 (3.3–7.5) | 2 | 4 | 1 | 1 |
| Subpectoral | 2 | 2 | 4.5 (4.4–4.5) | 0 | 2 | 0 | 0 |
| Supraclavicular | 3 | 3 | 6.5 (4.2–9.2) | 2 | 1 | 0 | 0 |
| Internal mammary | 2 | 2 | 5.5 (5.1–6.2) | 0 | 2 | 0 | 0 |

*Range is in parentheses.

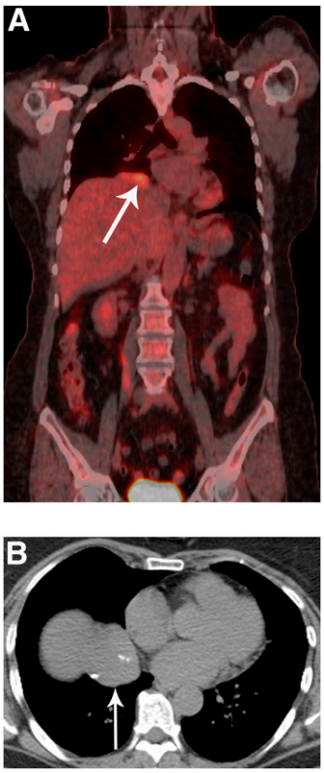


**FIGURE 4.** False-positive cardiophrenic angle mass in 59-y-old woman with biopsy-proven right IBC. (A and B) Coronal PET/CT (A) and axial CT (B) show 4-cm $^{18}$F-FDG–avid mass (maximum SUV, 5.2; arrows), with associated calcifications at cardiophrenic angle. Biopsy revealed reactive lymphoid tissue.

volume effects by providing more accurate information on lesion size that can be incorporated during PET image reconstruction or image analysis (*35*).

Nearly half the patients in our study (49%) had distant metastases at the time of initial staging, whereas metastases were reported in less than 10% of patients with small tumors (<2 cm) in the first 2 y after diagnosis (*36*).

Although 4 of 41 patients (10%) presented with clinical features of metastatic disease, in 7 of 41 patients (17%) PET/CT revealed distant metastases not known before PET/CT. One of these 7 patients had multiple sites of disease, and 6 had a single site of disease (1 confirmed on biopsy).

PET/CT detected bone metastases in 9 of 41 patients (22%), 3 of whom had negative WBS findings (2 lytic and 1 mixed lytic/blastic metastasis). In our study, 56% of patients with bone metastases had lytic metastases. In 1 patient with bone marrow metastases, MRI demonstrated more extensive disease in the vertebrae than did PET/CT, as is concordant with previous findings (*37,38*). Liver metastases were detected by PET/CT in 6 of 41 patients (15%). PET/CT accurately detected metastases in 3 patients with abdominal lymph node metastases (mesenteric and internal iliac lymph nodes) with a mean short diameter of 1 cm. PET/CT detected mediastinal nodal metastases in 24% of patients and contralateral nodal disease in 17% of patients.

A limitation of this study is that histopathologic findings were not available for all areas of abnormal hypermetabolism seen on PET/CT. This limitation is inherent to the retrospective nature of the study and reflects the standard treatment of patients with metastatic cancer (i.e., tissue diagnosis is performed only when a single metastatic lesion that may alter treatment is suspected). Patients with multiple sites of abnormal hypermetabolic uptake that are highly suggestive of widespread metastatic disease may not always undergo invasive biopsy, particularly when correlative anatomic imaging confirms features highly suggestive of metastatic disease and treatment needs to be expedited in the face of rapidly progressive disease.

## CONCLUSION

The preliminary results of this retrospective study demonstrate that PET/CT shows an exceedingly high percentage of ipsilateral axillary (90%), and subpectoral (44%) nodal (N3) disease. Nearly half the patients in our study (49%) had distant metastases at the time of initial staging, and 17% of distant metastatic lesions seen on PET/CT were clinically occult and not evident on baseline imaging. Eleven of the 20 patients (55%) with distant metastases in our study had disease in 2 or more organ sites. The large number of distant metastases in our study population may reflect the tertiary referral pattern at our institution and represents preliminary data that require further investigation. Although PET/CT is currently unable to allow clinicians to bypass all other imaging studies, further prospective studies are warranted to determine the validity of these preliminary findings. If validated, the cost of a PET/CT study in these patients may be equivalent to the total cost of imaging multiple organs and allow a single hospital visit and decreased imaging time, when compared with the time required for a battery of staging studies.

## ACKNOWLEDGMENTS

This study was presented in part at the 93rd scientific assembly and annual meeting of the Radiological Society of North America, November 25–30, 2007, and was supported in part by the Morgan Welch Inflammatory Breast Cancer Research Program.

## REFERENCES

1. Haagensen CD. *Diseases of the Breast.* 2nd ed. Philadelphia, PA: Saunders; 1971:576–584.
2. Cristofanilli M, Valero V, Buzdar AU, et al. Inflammatory breast cancer (IBC) and patterns of recurrence: understanding the biology of a unique disease. *Cancer.* 2007;110:1436–1444.
3. Yang WT, Le-Petross HT, Macapinlac H, et al. Inflammatory breast cancer: PET/CT, MRI, mammography, and sonography findings. *Breast Cancer Res Treat.* 2008;109:417–426.
4. Levine PH, Steinhorn SC, Ries LG, Aron JL. Inflammatory breast cancer: the experience of the surveillance, epidemiology, and end results (SEER) program. *J Natl Cancer Inst.* 1985;74:291–297.
5. Jaiyesimi IA, Buzdar AU, Hortobagyi G. Inflammatory breast cancer: a review. *J Clin Oncol.* 1992;10:1014–1024.
6. Fueger BJ, Weber WA, Quon A, et al. Performance of 2-deoxy-2-[F-18]fluoro-D-glucose positron emission tomography and integrated PET/CT in restaged breast cancer patients. *Mol Imaging Biol.* 2005;7:369–376.
7. Rosen EL, Eubank WB, Mankoff DA. FDG PET, PET/CT, and breast cancer imaging. *Radiographics.* 2007;27(suppl):S215–S229.

8. Tatsumi M, Cohade C, Mourtzikos KA, Fishman EK, Wahl RL. Initial experience with FDG PET/CT in the evaluation of breast cancer. *Eur J Nucl Med Mol Imaging.* 2006;33:254–262.
9. Fueger BJ, Weber WA, Quon A, et al. Performance of 2-deoxy-2-[F-18]fluoro-D-glucose positron emission tomography and integrated PET/CT in restaged breast cancer patients. *Mol Imaging Biol.* 2005;7:369–376.
10. Kumar R, Chauhan A, Zhuang H, Chandra P, Schnall M, Alavi A. Clinicopathologic factors associated with false negative FDG-PET in primary breast cancer. *Breast Cancer Res Treat.* 2006;98:267–274.
11. Wahl RL, Siegel BA, Coleman RE, Gatsonis CG, for the PET Study Group. Prospective multicenter study of axillary nodal staging by positron emission tomography in breast cancer: a report of the Staging Breast Cancer with PET Study Group. *J Clin Oncol.* 2004;22:277–285.
12. Gil-Rendo A, Zornoza G. García-Velloso MJ, Regueira FM, Beorlegui C, Cervera M. Fluorodeoxyglucose positron emission tomography with sentinel lymph node biopsy for evaluation of axillary involvement in breast cancer. *Br J Surg.* 2006;93:707–712.
13. Kumar R, Zhuang H, Schnall M, et al. FDG PET positive lymph nodes are highly predictive of metastasis in breast cancer. *Nucl Med Commun.* 2006;27:231–236.
14. Eubank WB, Mankoff DA. Evolving role of positron emission tomography in breast cancer imaging. *Semin Nucl Med.* 2005;35:84–99.
15. Isasi CR, Moadel RM, Blaufox MD. A meta-analysis of FDG-PET for the evaluation of breast cancer recurrence and metastases. *Breast Cancer Res Treat.* 2005;90:105–112.
16. Radan L, Ben-Haim S, Bar-Shalom R, Guralnik L, Israel O. The role of FDG-PET/CT in suspected recurrence of breast cancer. *Cancer.* 2006;107:2545–2551.
17. Avril N, Dose J, Janicke F, et al. Metabolic characterization of breast tumors with positron emission tomography using F-18 fluorodeoxyglucose. *J Clin Oncol.* 1996;14:1848–1857.
18. Taira AV, Herfkens RJ, Gambhir SS, Quon A. Detection of bone metastases: assessment of integrated FDG PET/CT imaging. *Radiology.* 2007;243:204–211.
19. La Fougere C, Hundt W, Brockel W, et al. Value of PET/CT versus PET and CT performed as separate investigations in patients with Hodgkin's disease and non-Hodgkin's lymphoma. *Eur J Nucl Med Mol Imaging.* 2006;33:1417–1425.
20. De Wever W, Meylaerts L, De Ceuninck L, Stroobants S, Verschakelen JA. Additional value of integrated PET-CT in the detection and characterization of lung metastases: correlation with CT alone and PET alone. *Eur Radiol.* 2007; 17:467–473.
21. Johnson MS, Gonzales MN, Bizila S. Responsible conduct of radiology research. Part V. The Health Insurance Portability and Accountability Act and Research. *Radiology.* 2005;237:757–764.
22. Elston CW, Ellis IO. *Assessment of Histologic Grade: The Breast.* Vol 13. New York, NY: Churchill Livingstone; 1998:356–384.
23. Greene FL, Page DL, Fleming ID, et al. *American Joint Cancer Committee Cancer Staging Manual.* 6th ed. New York, NY: Springer-Verlag; 2002:221–240.
24. Baslaim MM, Bakheet SM, Bakheet R, et al. 18-Fluorodeoxyglucose-positron emission tomography in inflammatory breast cancer. *World J Surg.* 2003;27: 1099–1104.
25. van der Hoeven JJM, Krak NC, Hoekstra OS, et al. $^{18}$F-2-fluoro-2-deoxy-D-glucose positron emission tomography in staging of locally advanced breast cancer. *J Clin Oncol.* 2004;22:1253–1259.
26. Lim HS, Yoon W, Chung TW, et al. FDG PET/CT for the detection and evaluation of breast diseases: usefulness and limitations. *Radiographics.* 2007; 27(suppl):S197–S213.
27. Avril N, Rose CA, Schelling M, et al. Breast imaging with positron emission tomography and fluorine-18 fluorodeoxyglucose: use and limitations. *J Clin Oncol.* 2000;18:3495–3502.
28. Fehr MK, Hornung R, Varga Z, et al. Axillary staging using positron emission tomography in breast cancer patients qualifying for sentinel lymph node biopsy. *Breast J.* 2004;10:89–93.
29. Levine PH, Steinhorn SC, Ries LG, Aron JL. Inflammatory breast cancer: the experience of the Surveillance, Epidemiology, and End Results (SEER) program. *J Natl Cancer Inst.* 1985;74:291–297.
30. Hance KW, Anderson WF, Devesa SS, Young HA, Levine PH. Trends in inflammatory breast carcinoma incidence and survival: the Surveillance, Epidemiology, and End Results program at the National Cancer Institute. *J Natl Cancer Inst.* 2005;97:966–975.
31. Bellon JR, Livingston RB, Eubank WB, et al. Evaluation of the internal mammary lymph nodes by FDG-PET in locally advanced breast cancer (LABC). *Am J Clin Oncol.* 2004;27:407–410.
32. Danforth DN Jr, Aloj L, Carrasquillo JA, et al. The role of $^{18}$F-FDG-PET in the local/regional evaluation of women with breast cancer. *Breast Cancer Res Treat.* 2002;75:135–146.
33. Mazziotta JC, Phelps ME, Plummer D, et al. Quantitation in positron emission computed tomography: 5. Physical–anatomical effects. *J Comput Assist Tomogr.* 1981;5:734–743.
34. Soret M, Bacharach SL, Buvat I. Partial volume effect in PET tumor imaging. *J Nucl Med.* 2007;48:932–945.
35. Hickeson M, Yun M, Matthies A, et al. Use of a corrected standardized uptake value based on the lesion size on CT permits accurate characterization of lung nodules on FDG-PET. *Eur J Nucl Med Mol Imaging.* 2002;29:1639–1647.
36. Veronesi U, Marubini E, Del Vecchio M, et al. Local recurrence and distant metastasis after conservative breast cancer treatments: partly independent events. *J Natl Cancer Inst.* 1995;87:19–27.
37. Hamaoka T, Madewell JE, Podoloff DA, Hortobagyi GN, Ueno NT. Bone imaging in metastatic breast cancer. *J Clin Oncol.* 2004;22:2942–2953.
38. Langsteger W, Heinisch M, Fogelman I. The role of fluorodeoxyglucose, $^{18}$F-dihydroxyphenylalanine, $^{18}$F-choline, and $^{18}$F-fluoride in bone imaging with emphasis on prostate and breast. *Semin Nucl Med.* 2006;36:73–92.